Simulation of Measuring Bottom Quark Flow in Heavy Ion Collisions Using the CMS Detector

by

Arthur James Franke

Submitted to the Department of Physics
in partial fulfillment of the requirements for the degree of

Bachelor of Science in Physics

at the

MASSACHUSETTS INSTITUTE OF TECHNOLOGY

June 2007

© Arthur James Franke, MMVII. All rights reserved.

The author hereby grants to MIT permission to reproduce and
distribute publicly paper and electronic copies of this thesis document
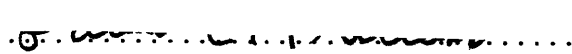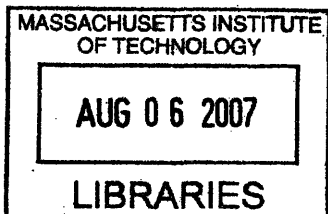in whole or in part.

Author ....
Department of Physics
May 11, 2007

Certified by...
Gunther Roland
Associate Professor
Thesis Supervisor

Accepted by...
David Pritchard
Undergraduate Supervisor, Department

Simulation of Measuring Bottom Quark Flow in Heavy Ion Collisions Using the CMS Detector

by

Arthur James Franke

Submitted to the Department of Physics
on May 11, 2007, in partial fulfillment of the
requirements for the degree of
Bachelor of Science in Physics

Abstract

In this thesis, I carried out a simulation study to characterize the measurement of bottom quark flow in relativistic Pb+Pb collisions using the Compact Muon Solenoid experiment. The Hydjet event generator is used to produce sample collision events at four centrality values between 0 and 12 fm. These events are processed using the simulation, digitization, and reconstruction modules of the CMSSW software framework. Studies of these data produce information necessary to create a flow signal simulator, and attempts are made at suggesting values for experimental cuts in p_T and DCA to reduce backgrounds. Using the signal simulator, it is determined that the muon elliptic flow coefficient, v_2^{μ}, varies linearly with that of open beauty, v_2^B, with the same constant of proportionality applicable in all background conditions. The expected statistical uncertainty of the flow measurement, RMS_{v2}, is shown to vary linearly with background level. Finally, RMS_{v2} is shown to vary with event sample size as predicted by background-to-signal ratio counting statistics.

Thesis Supervisor: Gunther Roland
Title: Associate Professor

Acknowledgments

There are a great many people whom I would like to thank, without whom this work would not have been possible. I apologize to anyone who may be unjustly forgotten in this section.

First, I would like to thank my advisor, Gunther Roland. I thank Prof. Roland for his help, guidance, ideas, and especially his patience throughout the thesis process. Without his encouragement, I would still know very little about programming, simulation, or heavy ion physics in general. Having worked with Prof. Roland in the classroom, during Junior Lab, and on this thesis, it is certain that his teachings have influenced my physics career.

I would also like to thank the members of the entire MIT Relativistic Heavy Ion group, in no particular order. Constantin Loizides for his patience in teaching a complete newbie how to program in C++ and ROOT. Maarten Ballintijn for the same qualities with regards to CMSSW. Yi Chen for providing the required data to do particle analysis. Burak Alver and Wei Li for simulation help. Brian Wilt for being in the trenches beside me. And Wit Busza for teaching me to never forget to ask "Why?."

I would like to thank my family for their support throughout my undergraduate career. My parents, Dr. Art and Sue Franke, for showing me the benefits that an education brings, and then providing me with the means to get a good one. My siblings, Rob and Liz Franke, for keeping me sane.

Last, but certainly not least, I would like to thank the brothers of the Massachusetts Γ Chapter of the ΦΔΘ Fraternity. *Εισ ανερ ουδεισ ανερ.*

Finally, I would like to formally dedicate this thesis to those teachers who inspired me to go farther: Mr. Jerry Stannard, Mr. Pittori, Mr. Charles Stannard, Mrs. Lisa Kriger, Ms. Linda Johansen, Mr. James Littlefield, Mr. James Buchan, Mr. Scott Mahon, Mrs. Holly Buckley, Mr. Daniel Briotti, Mrs. Rose Ann Hardy, Mrs. Claire Dahl, and Mr. David Seybold.

THIS PAGE INTENTIONALLY LEFT BLANK

Contents

List of Figures

10

THIS PAGE INTENTIONALLY LEFT BLANK

List of Tables

THIS PAGE INTENTIONALLY LEFT BLANK

Chapter 1

Introduction

Recent experiments at the Relativistic Heavy Ion Collider have provided a great deal of evidence for the existence of a liquid-like state of matter comprised of deconfined quarks and gluons, known as the Quark Gluon Plasma (QGP). One of the most striking properties of this bulk partonic matter is that of elliptic flow, where the participants in a non-central ion collision form a QGP which does not expand isotropically, but rather favors expanding along the minor axis of the elliptical interaction zone. In studies thus far, one key probe for studying the QGP has been observing how heavy flavors of quarks, namely charm and bottom, are affected by the outward anisotropic flow of the medium. Heavy quarks are especially valuable in such studies, as they are the only particles to carry information about the QGP from the very instant it is created. Due to the nature of the medium, a unique physical system arises where bound states of heavy quark $q\bar{q}$ pairs, called quarkonia, are more frequently split up to produce in mesons containing only one heavy quark. In addition to effects like jet suppression, this decrease in the frequency of quarkonia production is a key indicator of the nature of the QGP.

Until now, measurements of heavy quark flow have been either unable to distinguish between the c and b flavors, or have only focused on the more-accessible properties of open charm production. However, with the arrival of the higher energies available at the Large Hadron Collider, it will be possible to specifically observe how bottom quarks interact with the QGP, and how the production of open bottom

mesons is affected by the partonic medium.

In this study, simulated data of ion collisions at LHC energies will be used to characterize the spectrum of muons produced when these open B mesons decay via semileptonic channels, and describe how the Compact Muon Solenoid detector can be used to make a measurement of b-quark flow using this decay channel. Chapter 2 of this work will present a brief overview of some of the theory behind how bottom quarks are produced in the QGP, how open bottom mesons are formed via screening processes, and how elliptic flow of the QGP causes their emission to be anisotropic in the azimuthal direction ϕ. Chapter 3 will give an overview of the CMS detector and the detector subsystems which are vital to observing the flow and decays of B mesons. Chapter 4 will describe the method of analysis used to characterize b-quark flow in heavy ion collisions using Monte Carlo sample data. Chapter 5 will show how this analysis was used to construct a simulation of what the B flow signal will look like in actual data, and how the signal is affected by changes in the relevant flow parameters. Finally, Chapter 6 will summarize the conclusions of this study by outlining conditions for a successful measurement of b-quark flow using the CMS detector.

Chapter 2

Beauty Production in Heavy Ion Collisions

2.1 Overview

The production of bottom quarks has been studied ever since the discovery of the $b\bar{b}$ resonance at 9.5 GeV in dimuon collisions, discovered experimentally in 1977 at Fermilab [1]. Today, this is known as the Υ particle, or "bottomonium." Open-beauty mesons, or a meson with only one b-quark and a quark of a lighter species, were discovered in 1980 at the Stanford Linear Accelerator Center [2]. In the past nearly 30 years, collider experiments involving two particles have served to establish the branching ratios of the different heavy mesons [3]. Today, theory is able to accurately predict cross sections for beauty production using perterbative quantum chromodynamics [4]. With the advent of heavy ion studies where collision energies are such that heavy flavor production is measurable, deviations from typical production cross-sections of heavy quarkonia have been observed [5, 6]. It is thought that this observed suppression of $q\bar{q}$ states in favor of open flavor mesons is evidence of the effects of flavor screening within the QGP [7], a mechanism which will be explained in greater detail below. Since the bottom quark is the heaviest quark species capable of substantial strong interactions with nearby particles, it is an important probe for studying flow of particles within the QGP.

2.2 *B* Meson Characteristics

A B meson is a hadron consisting of one b or $\bar{b}$ quark in a bound state with another, lighter-flavor parton (see Table 2.1 for a listing and properties of the B mesons). Hadrons containing a $b\bar{b}$ pair are termed bottomonium, or Υ particles [8]. Bottomonium states are referred to as "closed beauty," while B mesons are known as "open beauty." In the framework of the vector mesons, open beauty is known to have a nonzero beauty quantum number $(B = \pm 1)$, while closed beauty is in a zero-beauty quantum state $(B = 0)$. This quantum number has implications on the creation of beauty systems: it must be conserved in strong processes, so for every b produced a $\bar{b}$ must also be produced.

Table 2.1: Properties B mesons. Adapted from [3].

Species	Quarks	Mass [Mev]	Mean Life τ [ps]	$c\tau$ [μm]
B^+	$u\bar{b}$	5279.0 ± 0.5	1.636 ± 0.011	491.1
B^-	$\bar{u}b$	5279.0 ± 0.5	1.636 ± 0.011	491.1
B^0	$d\bar{b}$	5279.4 ± 0.5	1.530 ± 0.009	458.7
$\bar{B}^0$	$\bar{d}b$	5279.4 ± 0.5	1.530 ± 0.009	458.7
B^0_s	$s\bar{b}$	5367.5 ± 1.8	1.466 ± 0.059	439
$\bar{B}^0_s$	$\bar{s}b$	5367.5 ± 1.8	1.466 ± 0.059	439
B^+_c	$c\bar{b}$	6286 ± 5	$0.46^{+0.18}_{-0.16}$	140
B^-_c	$\bar{c}b$	6286 ± 5	$0.46^{+0.18}_{-0.16}$	140

Useful to this study is the high likelihood of a B meson to decay in a process where one of the products is a lepton, known as a semileptonic process. In these interactions, the b quark involved emits a $W^\pm$ boson, thereby changing its weak isospin and turning into a lighter-flavor quark. The $W^\pm$ then decays into a lepton, which is detectable, and the corresponding neutrino in order to conserve lepton number [8]. An example Feynman diagram for a semileptonic b decay process is shown in Figure 2-1. Past heavy-ion experiments have made extensive use of the $e^\pm \nu_e$ decay channel for studying heavy quark flavors [9, 10, 11]. However as collision energies increase and decay muons are produced with enough energy to be experimentally viable, the $\mu^\pm \nu_\mu$ channel becomes accessible for measurements. For an admixture of B mesons typically

18

found in open beauty production events, the decay channel $(B^{\pm}/B^0/B^0_S/b-$baryons$)$ $\rightarrow \mu^{\pm}\nu_{\mu}+$ anything occurs $(10.95^{+0.29}_{-0.25})\%$ of the time [3]. This branching fraction is approximately the same as for semileptonic decays to electrons, making the muon channel of similar statistical use.
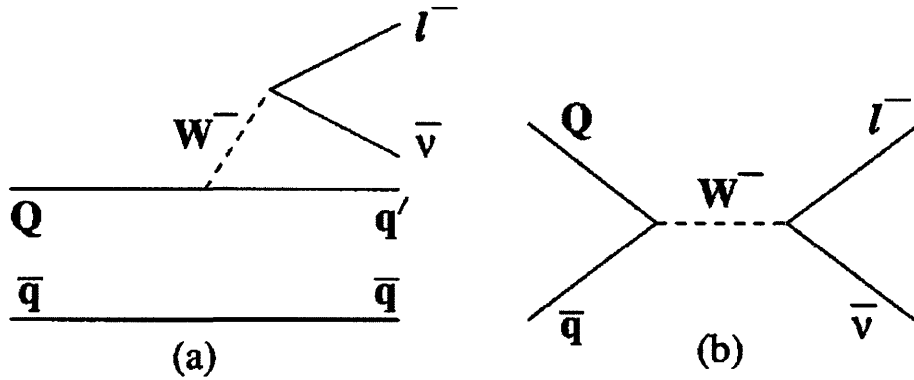
Figure 2-1: Feynman-diagram examples of open-flavor mesons decaying by (a) semileptonic and (b) leptonic processes. Adapted from [12].

2.3 Meson Formation in the QGP

Due to their large 4.5 GeV mass, b-quarks are primarily formed only in hard-scattering collisions between nucleons, through one of three processes: pair creation, flavor excitation, or gluon splitting [4]. When created, the quarks must be initially in a $b\bar{b}$ state, due to the requirement that the beauty quantum number is conserved in strong interaction processes. Open beauty arises when the quarkonia interact with neighboring particles, allowing the constituent b quarks to bind with local quarks of lighter flavors. In the dense partonic matter of the QGP the effect of color charge screening on the bound quarkonia accelerates this process, resulting in a suppression of quarkonia resonances in favor of heavy quark mesons above levels found in pp collisions. The measurement of this suppression effect, the nuclear modification factor R_{AA}, has been predicted for expected values of flow parameters [13]. Accurate measurements of B meson production and flow may validate these nuclear interaction models.

2.4 Elliptic Flow of the Quark-Gluon Plasma

The majority of heavy ion collisions are peripheral (for instance, see Figure 5-1), leading to an area of interaction shaped somewhat like an ellipse where the two nuclei geometrically overlap. It is inside this region where nucleon-nucleon collisions occur, and where the QGP is formed at temperatures and pressures many times higher than normal nuclei. These pressures force the QGP to flow outwards in a manner indicative of the equation of state of the plasma [14]. Early experiments showed that particles emanating from ion collisions were emitted anisotropically in the azimuthal angle ϕ, with more particles emitted along the plane parallel to the beam path and to the impact parameter vector of the collision, known as the reaction plane [15]. This behavior is known as elliptic flow, where the medium produced in the collision expands more quickly outward along the direction of the reaction plane, or the semi-minor axis of the elliptical interaction region [16]. Theoretical models combining the hydrodynamic effects of a liquid with strong particle interactions have showed this effect to sensitive to th equation of state of the QGP [17].

In practice, elliptic flow is measured to the degree of anisotropy found in particle production in ϕ relative to the reaction plane of each collision. This can be quantized in terms of a Fourier expansion of ϕ-space distributions:

$$\frac{dN}{d\phi} = 1 + 2v_2 \cos 2\phi \qquad (2.1)$$

where v_1 and v_2 are the coefficients of the Fourier terms. Elliptic flow is present when v_2 is nonzero. Such measurements of v_2 can be made using studies of single particle multiplicities [18], centrality dependences of particle production [19], as well as impacts upon the spectra of particles in pseudorapidity, centrality, p_T, and center-of-mass energy [20]. These measurements have shown the effects of elliptic flow to be in agreement with hydrodynamic models of the QGP behaving as a strongly-interacting liquid [21].

2.5 Comparison to Υ Channels

Comparison of meson and quarkonia production rates serves as an accurate probe of the thermal properties of the QGP after creation. Such comparisons involving the J/ψ particle and D mesons have already been used as evidence for formation of the QGP [7]. Theory predicts that similar measurements of the $\Upsilon/\Upsilon'/B$-meson multiplicities will give us large amounts of information about how the QGP thermalizes and behaves in the initial time after the collision [22]. Thus, accurate measurements of B meson multiplicity and flow are of great interest to studies of QGP thermalization.

2.6 Results of Previous Studies

The collision energies accessible at the LHC provide this study with a unique opportunity: previous studies have generally lacked the collision energy to make muons a useful method of heavy flavor detection, as well as lacked the energy to allow a study to be focused specifically on B mesons separately from other heavy flavors. Studies using muons have been undertaken for charm production [23]. Many studies have used electrons to examine heavy quark flow, considering charm and beauty simultaneously [9, 10, 11]. Their results indicate a nonzero flow term v_2 in the range $0.03 \leq v_2 \leq 0.1$ for $0.5 \leq p_T \leq 3.5$ GeV [18]. Studies using LHC and CMS will extend these measurements to higher ranges of p_T, as well as permit the examination of open beauty flow independently of charm.

THIS PAGE INTENTIONALLY LEFT BLANK

Chapter 3

The CMS Experiment

3.1 The Large Hadron Collider

Expected to be operational in late 2007, the Large Hadron Collider, located at CERN outside of Geneva, Switzerland, will provide the premier facility for studying particle and ion interactions at high energies. The first beams will be of protons, at energies of only $\approx$400 GeV to provide an opportunity for engineering diagnostics and detector calibration studies to occur [24]. Some time in 2008, the first full-energy pp beams will be attempted, with collisions occurring at the design specification of 14 TeV center of mass energy. During each calendar year, 8 months of operation will be dedicated 'to pp collisions, while one month out of every year will be dedicated to heavy ion physics. There is a low-energy, low-luminosity engineering run planned for heavy ions, similar to the 400 GeV pp calibration run. When colliding heavy ions at full specified capabilities, the LHC will provide capabilities for collision energies of up to 5.5 TeV per nucleon, with luminosities of $10^2 7$ cm^{-2} s^{-1} at an interaction rate of one event every 99.8 ns [3].

Around the 27 km-circumference LHC ring are situated four active experimental halls, or interaction points. These four IP's are home to the LHC experiments: CMS, ATLAS, ALICE, and LHCb. CMS and ATLAS (A Toroidal LHC ApparatuS) [25] are general-purpose experiments, designed primarily for pp studies, but each with capabilities for heavy ion studies. ALICE (A Large Ion Collider Experiment) will

focus primarily on heavy ion physics [26], while LHCb will examine beauty physics in pp collisions [27].

While there is a dedicated heavy ion experiment planned for the LHC, the CMS detector is capable of making some measurements critical to heavy ion studies to better levels of precision than ALICE. ALICE intends to make the majority of its measurements relying upon hadronic particle production channels to give information about the QGP. CMS will provide a more precise system for tracking and measuring leptons produced in collisions, as well as a higher-resolution electromagnetic calorimeter for determining particle kinematics. The CMS detector is also designed to provide better coverage in many regimes of ϕ and η for leptonic channels. Thus, for the purposes of this study, CMS is the superior detector to be measuring B flow using semileptonic decay channels.
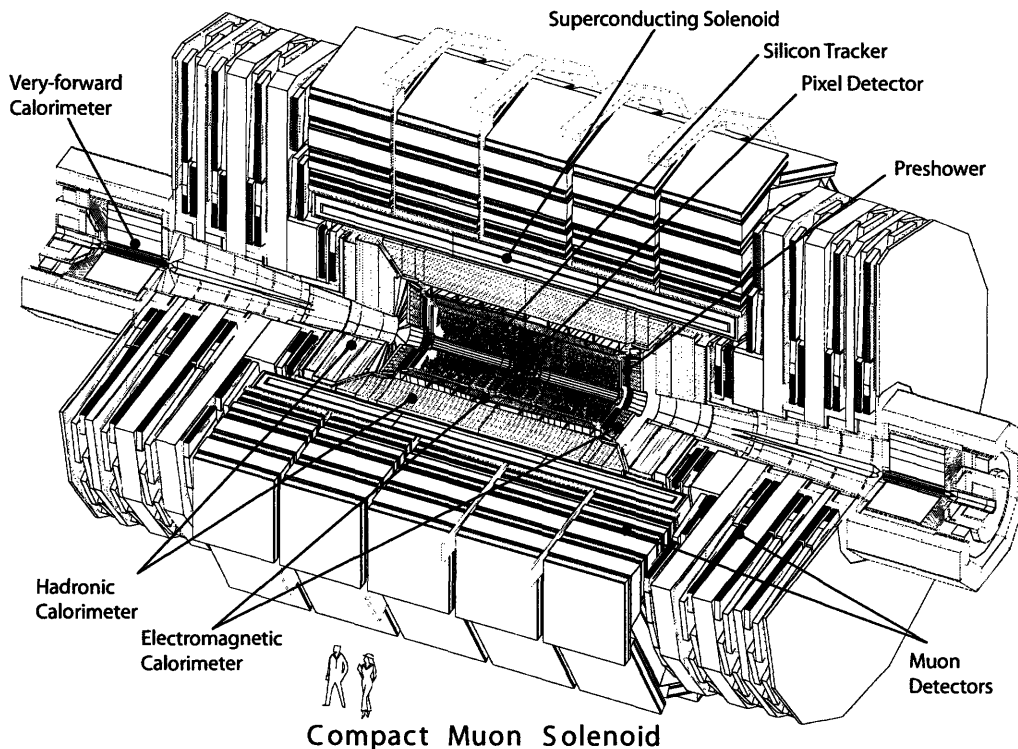
Figure 3-1: An engineering rendering of the CMS detector, with cut-away view to show detector subsystems. People shown for scale, not true color. Adapted from [28].

24

3.2 CMS Detector Description

The Compact Muon Solenoid detector is a general-purpose collider experiment designed primarily to study pp collisions [29]. However, its robust hardware also provides the high level of particle acceptance, as well as the precision tracking and momentum determination necessary to effectively study heavy ion events [30]. The detector (rendering shown in Fig. 3-1) is build around a large superconducting solenoid, which provides an internal field strength of 4 T. Within the bore of the magnet is housed a silicon tracker (pixel tracker and strip tracker), electromagnetic calorimeter (ECAL), and hadronic calorimeter (HCAL). Outside the magnet are the muon spectrometer, and an iron field return yoke. In its entirety, the cylindrical detector measures 21.6 meters long by 14.6 meters in diameter, and weighs 12,500 tonnes [29]. While CMS is not the largest of the LHC detectors, it is the heaviest.

3.3 Relevant Detector Subsystems

This study relies primarily on two detector subsystems of the CMS detector: the muon spectrometer, and the silicon tracker. The muon spectrometer is the only component of the detector capable of reliably identifying the high-energy muons produced from heavy flavor decays. The tracker system is also specifically vital to studies of B meson production, as secondary vertex reconstruction and location is necessary to distinguish the desired secondary particle decay vertices from background decays originating from the primary vertex.

3.3.1 Muon System

The CMS Muon System is the subsystem around which the rest of the apparatus has been designed [31]. It is designed primarily to measure the signature four-lepton decay of the Higgs Boson $H \rightarrow ZZ \rightarrow 4\mu^{\pm}$ in pp collisions, though its capabilities lend it to precisely exploring any physics involving high-p_T muons.

Taking advantage of the penetrating nature of muons, the muon system is located

outside of the solenoidal magnet, within the iron flux return yoke. This configuration places ≈16 radiation lengths of material between the interaction point and the muon system, greatly reducing the likelihood of hadronic backgrounds entering the muon system. As muons leave the interaction point, they are bent by the solenoidal field, changing direction once they leave the bore of the magnet. This pattern of motion allows spatial tracking of the muon to give information about the particle's charge and kinematic parameters. CMS exhibits the most precise capabilities for determining muon momentum, with one of the largest detector acceptances (full coverage in ϕ, up to $\eta = 2.4$, large p_T range) [32].

The constituent detector elements of the muon system are chosen to provide complementary measurement capabilities, thereby increasing measurement accuracy. Resistive Plate Chambers (RPCs) offer a fast-triggering capability, while Drift Tubes (DTs) and Cathode Strip Chambers (CSCs) give precise spatial measurement capability. The element layout (shown in Figure 3-2) uses DTs in the barrel section of the detector ($\eta \leq 1.2$), and CSCs in the endcap portions ($0.9 \leq \eta \leq 2.4$), with RPCs adjacent to both sets of components on the side towards the interaction point. Combined, these systems provide an expected reconstruction efficiency of greater than 95% [33].

3.3.2 Silicon Tracker

The CMS Silicon Tracker [34] uses a combination of silicon pixel detectors and silicon strip detectors to accurately track the locations of particles as they leave the region within the beam line. It has been designed to perform in an environment of high magnetic field and high radiation, as is found closest to the CMS interaction point. The tracker is divided into two parts (layout shown in Figure 3-3): the inner barrel (TIB) and outer barrel (TOB) structures [35]. The TIB is comprised of four inner barrel shells, with two layers of inner endcap layers (TIE). The TOB is made up of six barrel layers, with two outer endcaps providing seven layers of detector panels. This configuration provides tracking up to $|\eta| \leq 2.5$, and full coverage in ϕ.

Important to this study is the tracker's ability to reconstruct the distance between
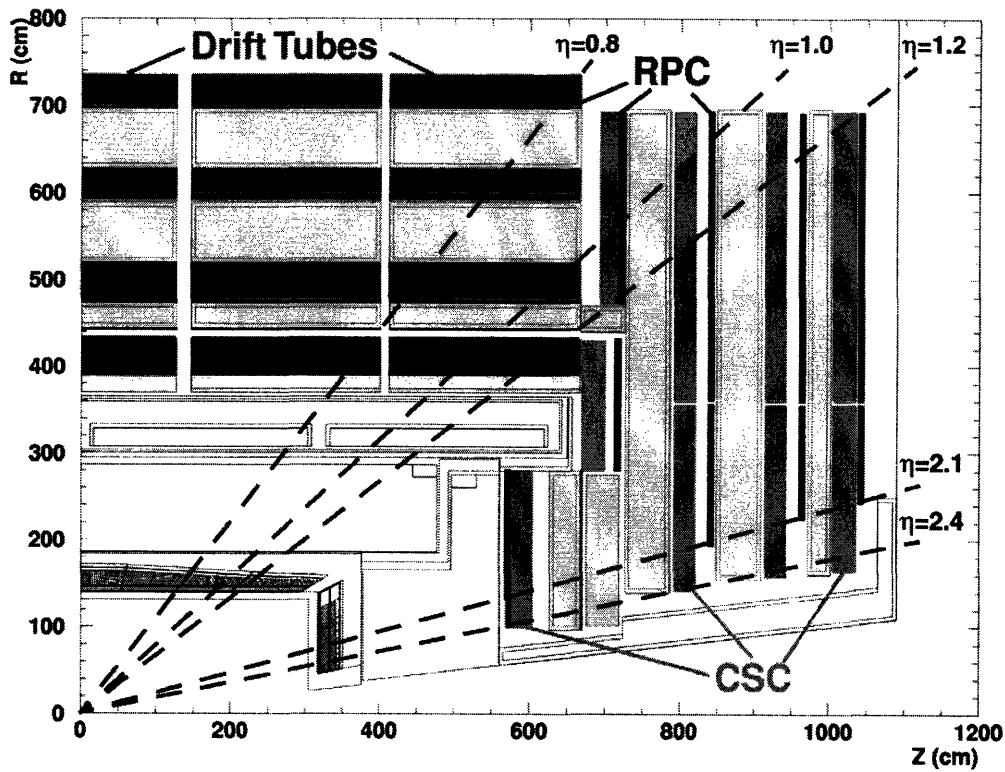
Figure 3-2: An engineering rendering from [33] providing a cross-sectional view of one quadrant of the muon system, with labeled detector elements. Dotted lines show points of interest in the muon system's coverage in pseudorapidity η.
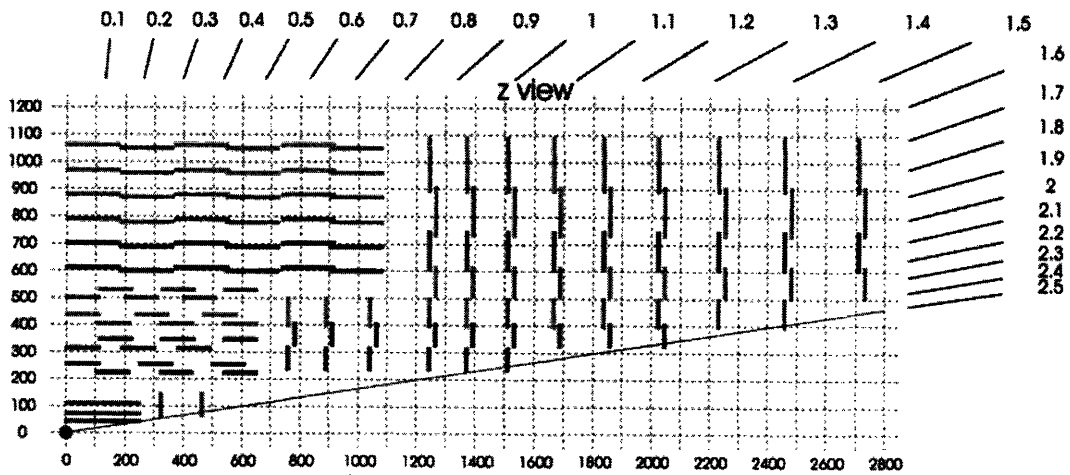
Figure 3-3: A drawing of one quadrant of the CMS Silicon Tracker layout, in cross-sectional view. Measurements along the vertical axis are radial distance from the beam line, and measurements along the lower horizontal axis are distance from the interaction point, both in mm. Numbers along the upper edge show coverage in pseudorapidity η. Adapted from [35].

27

the track of a single muon from a possible B meson decay and the main collision vertex. In many sources this measurement is called z-coordinate impact point z_{imp}, or distance of closes approach (DCA): in this study it will be referred to by the latter term. B mesons have a characteristic decay length $c\tau$ known to be on the order of 475μm [3]. Most sources of background for the high-p_T muons being examined in this study come from decays within the central vertex of the QGP, or originate from secondary vertices produced by D meson decays at a decay length $c\tau_D \approx 300\mu$m. Thus, to be useful as a background veto mechanism, tracking must have a DCA resolution less then the difference in decay lengths $c(\tau_B - \tau_D) \approx 200\mu$m (for an admixture of D and B meson species). Simulation studies [36] have shown this to be possible for single muons with full detector coverage in η for energies up to 10 GeV, and with adequate coverage for higher energies. This is well within the limits for expected muon p_T spectra. Thus, the CMS silicon tracker will be invaluable for reducing backgrounds in single muon studies of open beauty.

3.4   Improvements over RHIC

The pairing of the CMS experiment with the LHC will provide two significant advantages over previous experiments carried out at RHIC. First, the LHC will provide ion collisions of high enough energy density to make a study of open beauty production feasible, as well as differentiable from studies of charm. Second, the LHC-CMS combination will allow muons to be used as a primary probe of heavy quark flow. While some studies of heavy quarks were carried out on RHIC-era detectors involving muons (for instance, [23]), this decay channel was not energetic enough to be separable from hadron backgrounds. Thus, most studies of heavy quark flow at RHIC using semileptonic channels were carried out using electrons. Essentially, this combination of machine and detector will enable studies with muons to be successful at a level never seen before.
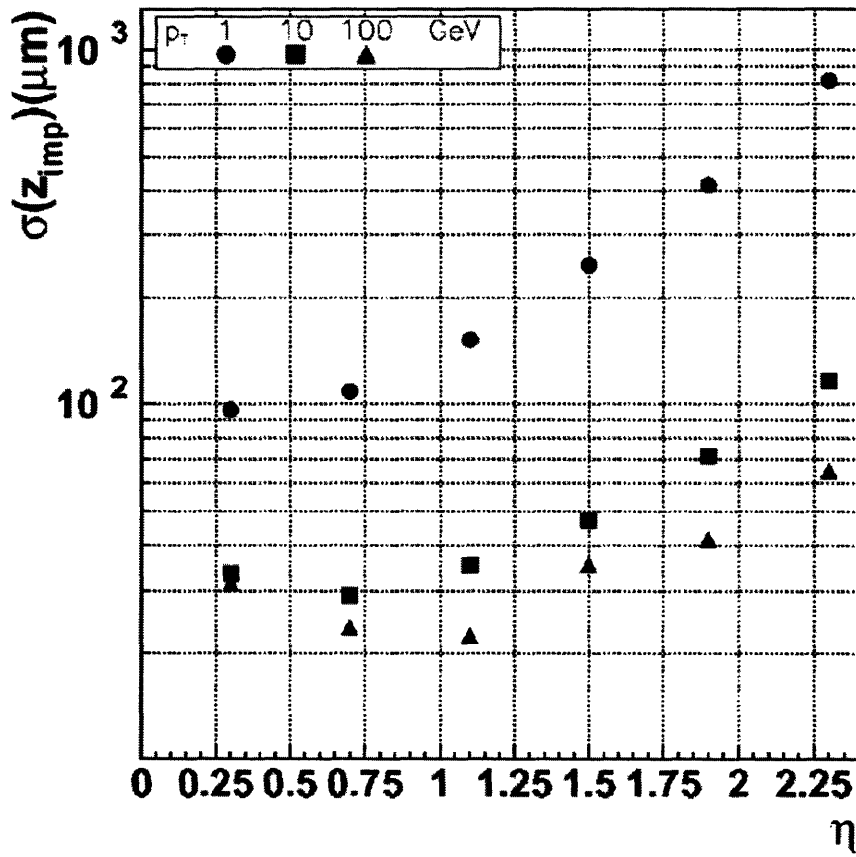
Figure 3-4: A plot showing the resolution for the z-coordinate impact point z_{imp} of single muons using the CMS Silicon Tracker, for different values of $|\eta|$ and p_T. Adapted from [36].

THIS PAGE INTENTIONALLY LEFT BLANK

Chapter 4

Monte Carlo Data Analysis

4.1 Hydjet Simulation

Since he LHC will not come online until late 2007, with the first heavy ion beams not occurring until some time in 2008, for this study it is necessary to employ a Monte Carlo method to provide simulated data for ion collisions at energies appropriate to the LHC. This method should take into account the elliptic flow already seen at RHIC, as well as provide accurate cross sections for particles which will be more accessible at LHC energies than they were during RHIC studies, such as heavy quarks. For this study, the Hydjet event generator package was used [37]. Hydjet employs the HYDRO flow-effect generator, the Pythia 6.4 particle collision generator, and the PYQUEN jet-quenching model to generate a fairly accurate portrayal of a heavy ion event.

To generate particles produced in hard scattering interactions between nucleons, Hydjet calls the *pp* event simulation package Pythia 6.4, filling a number of vertices with individual Pythia events. The number of vertices filled is dependent upon the impact parameter specified for the event. These vertices are the main source of the *b*-quarks relevant to this study, as the soft component of the simulation does not treat such heavy particles. However, due to the single-collision nature of each Pythia vertex, this also results in an isotropic distribution of heavy flavor, opposed to the elliptic flow-dependent signal with nonzero v_2 which will be studied once actual experimental

Table 4.1: Properties of the Hydjet-generated HEP-MC data set used to characterize particle production parameters. Data set provided by [38].

Impact Parameter [fm]	Events	Average Event Size [MB]
0	851	196
4	969	133
9	9,410	35.2
12	94,900	5.65

data is required. Unfortunately, neither the HYDRO or PYQUEN component of Hydjet simulate this effect. Since the intent of this study is only to characterize the muon spectrum, an isotropic distribution in ϕ is acceptable (flow effects will be added manually for construction of a sample signal in the next section).

For this study, four sets of generated events were used, with each set representing collisions at a specific impact parameter: $b = \{0, 4, 9, 12\}$ fm [38]. Since more central events produce orders of magnitude more particles, and thus much larger data files, an equal number of events was not practical. However, this effect is slightly offset by the fact that more central events have a higher probability of producing the B mesons of interest to this study due to the larger number of binary nucleon-nucleon collisions. The numbers of events for each centrality bin are shown in Table 4.1.

4.2 The CMSSW Framework

Analysis of the data generated with Hydjet was performed using the CMSSW 1.3.2 software framework [39] combined with the ROOT 5.15/06 data analysis framework [40]. This will permit easy application of the developed analysis methods to actual experimental data once it becomes available. For the purposes of this study, the CMSSW framework is also crucial to completing simulations of how events are detected within the CMS apparatus.

Sample data produced using the Hydjet event generator are put through three main steps of processing before analysis: simulation (SIM), digitization (DIGI), and reconstruction (RECO). The SIM stage uses a Geant4 algorithm to trace particle

Table 4.2: Results from determining the frequency of occurrence of open beauty in the MC Truth data set.

Impact Parameter [fm]	N_{Events}	N_B	N_B/event
0	851	18291 ± 135	$21.49 \pm .16$
4	969	13960 ± 118	$14.41 \pm .12$
9	9410	31347 ± 177	$3.331 \pm .019$
12	94900	26268 ± 162	$0.277 \pm .002$

tracks through the CMS detector, taking into account the magnetic field and geometry of the various detector components. The DIGI stage uses information produced by the SIM algorithms to produce a set of simulated subdetector responses. These are the signals which would be produced by the CMS electronics for the given particle tracks. In some cases, the RECO step is then performed, using framework-standard algorithms to reconstruct and tag particles based on the DIGI data. In this study, only muon reconstruction is used. It should be noted that due to the higher particle multiplicity versus pp collisions that is intrinsic to central heavy ion collisions, RECO steps were only successful on $b = 12$ sample events. Since not all reconstruction algorithms designed for heavy ion use have been implemented in CMSSW at the time of writing, in the future such tools should be available. For many statistical analyses of particle production, only the SIM and DIGI steps are required, as MC Truth data is accessible without running the time-consuming RECO step.

4.3 Single Muon Event Analysis

In this analysis, the goal is to select and study events from the simulated data in which muons are produced, with the muons coming from the semileptonic decay of B mesons. To accomplish this, analyses of both the simulated MC Truth data and the RECO data are used.

The first analysis executed using the MC Truth data are performed to place estimates on the frequency of open beauty production in collision events. Theoretically, b production should occur with higher frequency in more central collisions, as there
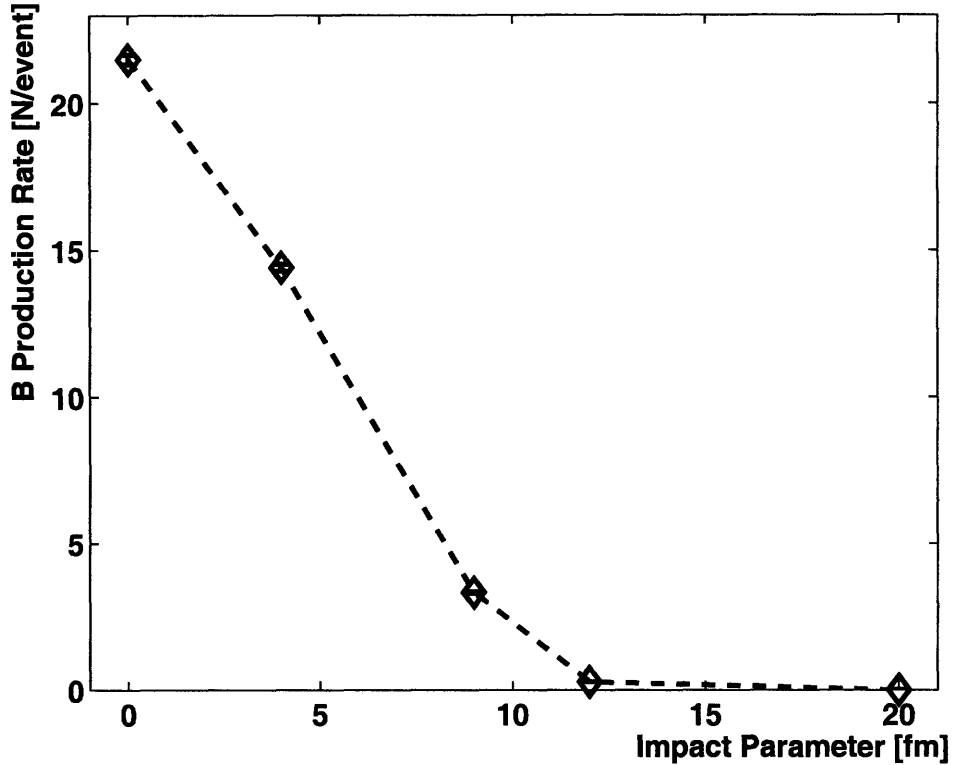
Figure 4-1: Plot showing B meson production rates versus impact parameter as determined using the Hydjet-generated MC Truth data. The dotted line shows the piecewise-linear interpolation function used in the flow signal simulation study.

are more hard-scattering events with sufficient energy. The measurement was taken by simply searching through all particles in the MC Truth data and selecting those particles with a PDG-standard Particle ID matching one of those found in Table 2.1. The results are shown in Table 4.2. For use in later studies, these data were parameterized to first-order in a piecewise linear function, shown in Figure 4-1. The validity of these data may be suspect: previous estimates [41] for $b\bar{b}$ pair production at $b \approx 3$ fm, presuming a near-unity conversion to open beauty due to color screening, place the maximum production rate at ≈ 9 mesons per event. However, later in this study simulation methods will be parameterized for an arbitrary number of B's produced, thus this error factor will only be of concern when real data comes online.
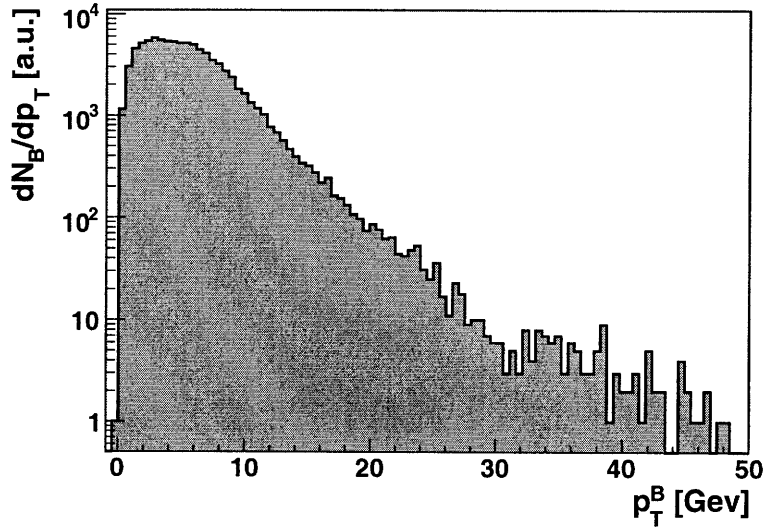
Figure 4-2: Spectrum of p_T^B for mesons generated by Hydjet, used to pseudo-randomly generate momenta of mesons for the flow signal simulation. Compare to [42].

In addition to production rates, the p_T spectrum of the B mesons was also recorded for each impact parameter value. This data will be used later in the flow signal simulation to help determine the relationship between the B elliptic flow signal and the observable ϕ_μ signal. The spectra for each impact parameter bin were found to be very similar in shape, with no parameterizable differences between them. Thus, the data sets were summed to produce a single spectrum in p_T, shown in Figure 4-2. In actual data from heavy ion collisions, a small variation of the p_T spectrum with centrality is expected, but should not be of enough significance to affect the results of this study.

Next, it was necessary to determine what percentage of the MC Truth B mesons decayed to muons, as well as the rate of muons produced by background channels. The first task was carried out by using known B mesons within the data set, found by the method described above, and selecting any muons found within their chain of daughter particles. Remaining muons in the data which hadn't been tagged as products of B decays were then assumed to be background muons. The total spectrum of muons can be seen in Figure 4-3.
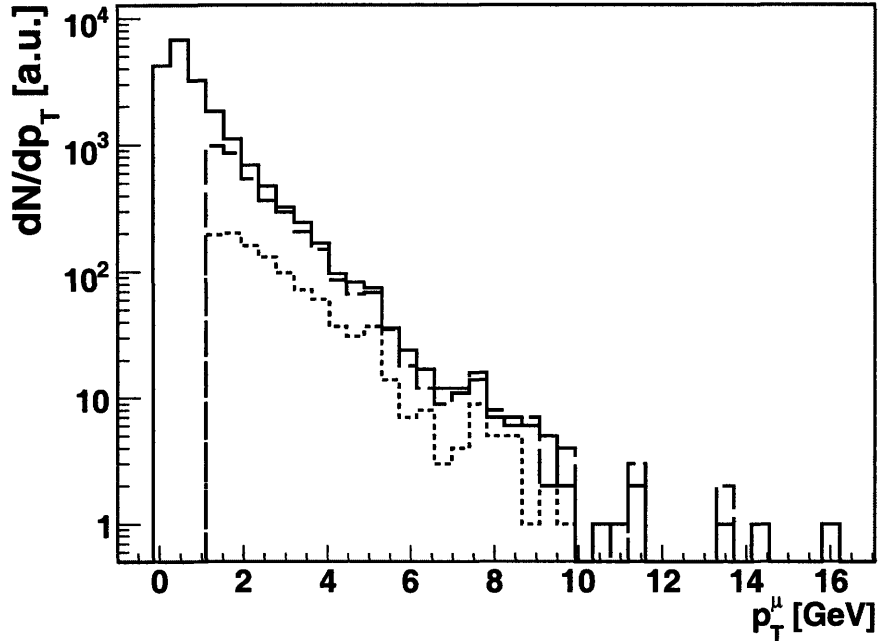
Figure 4-3: Distributions of muons in the Hydjet-generated MC Truth data. Black line is all muons, with total acceptance. Red line is all muons, with geometric and kinematic acceptance cuts imposed. Blue line is muons from B meson decays, with geometric and kinematic acceptance cuts imposed.

It should be noted that all muons so far have been selected from the raw simulation data without any other chriteria but particle ID matching, and thus consider candidates in all ranges of p_T, η, and ϕ. In practice, the detected spectra would be different, as the geometry and composition of the CMS detector render muons with p_T and η parameters below a certain threshold undetectable. For example, muons with too high a pseudorapidity would exit the detector close to the beam line, never having impacted a detector channel, while a muon with too low a p_T at midrapidity would take too tight a helical path in the solenoidal field to ever enter the muon detectors. Previous simulations have established the parameters of these kinematic cuts [32], and a simplified piecewise-linear model has been used for this study. An illustration of the kinematic threshold used, along with the data used to establish it, can be seen in Figure 4-4. Since abiding by these kinematic cuts is necessary for accurate simula-
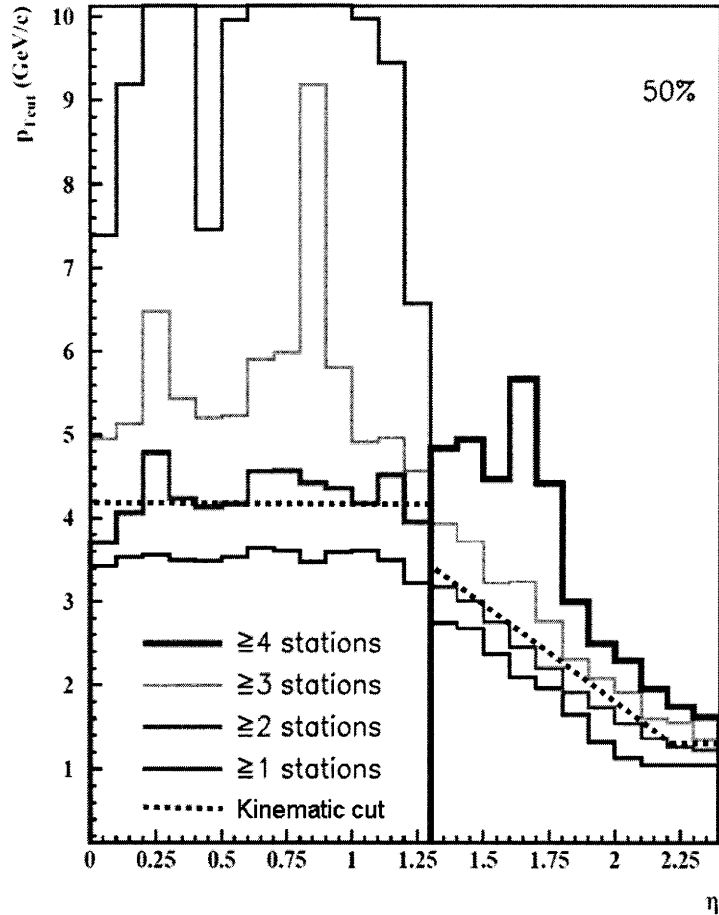
Figure 4-4: Data from [32] indicating p_T thresholds of single muons as a function of η at average acceptance. The dashed line indicates the piecewise-linear threshold used in single muon analysis.

tion of data produced in typical detector performance, they are used in producing all subsequent results (i.e. when production rates of muons are considered). The impact of these kinematic cuts on the muon spectrum can be seen in Figure 4-3 for both signal and background muons. Within detector acceptance, it this data indicates that a signal decay muon is produced with a probability of $P_\mu = 0.01213$. Additionally, the ratio of background muons to signal muons was found to be relatively constant across all values of impact parameter b, with an average value of 1.875 background muons per signal muon within detector acceptance.
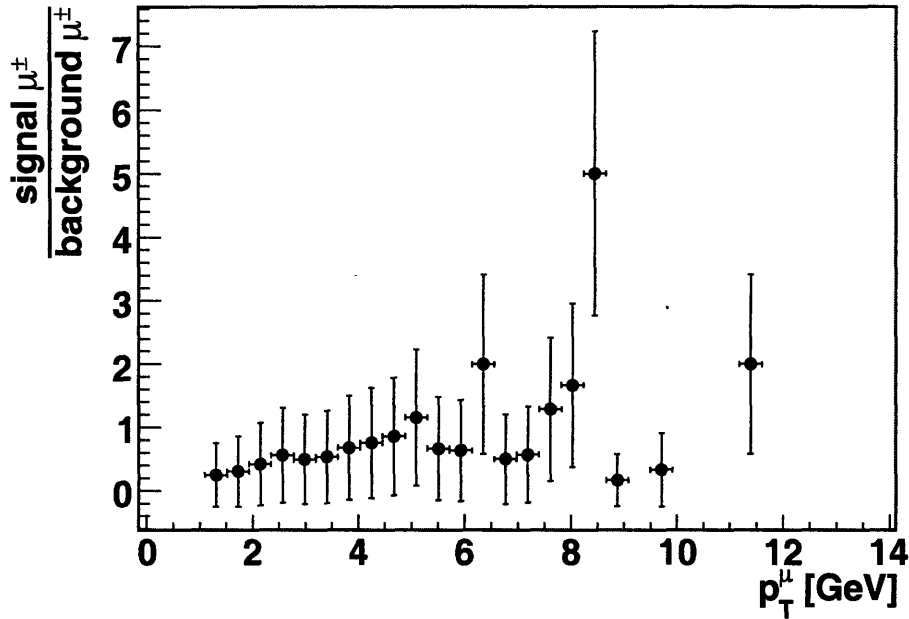
Figure 4-5: Plot showing the ratio of signal muons to background muons as a function of p_T, generated from MC Truth data. Error bars show statistical variation: limited counting statistics and resulting large uncertainties prevented use of this data in the single-muon analysis.

4.4 Transverse Momentum Cutoff Study

An attempt was made to use the p_T spectra from signal and background muons to establish a further cut in p_T to improve signal to noise. Muons originating from beauty decays are more likely to dominate the spectrum at higher values p_T, thus there should exist a regime above a certain value where the signal to noise is inherently greater than one. A comparison of the signal and background muon spectra, shown in Figure 4-5 showed no distinct value of p_T where a cutoff isolate an area of better measurement performance. Statistical errors for these data were large due limitations on the data set, so with further event generation this measurement may still be possible.
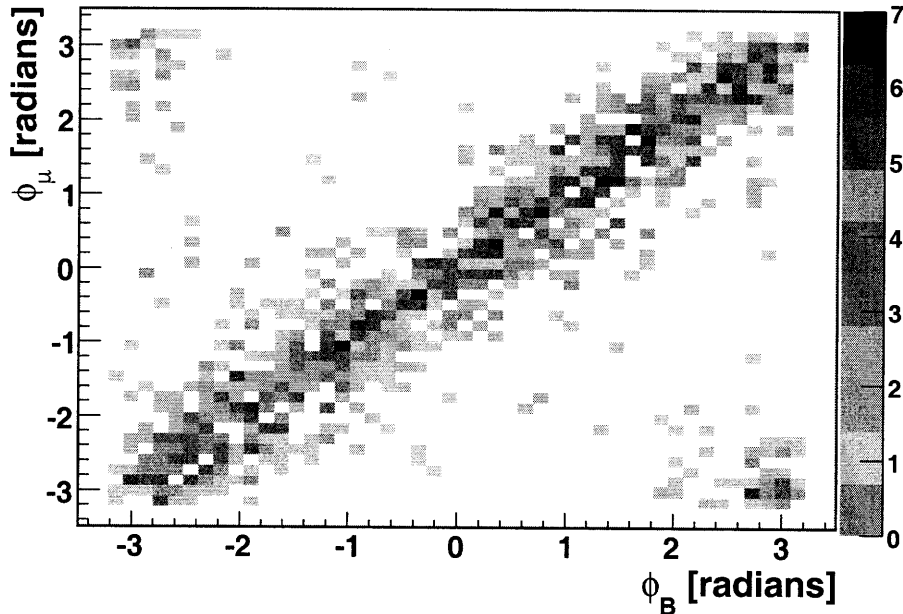
Figure 4-6: Two-dimensional histogram showing values of ϕ_B and ϕ_μ for all corresponding $B \to \mu^\pm$ mother-daughter pairs. A total of 1,090 mother-daughter pairs are tabulated, including the entire spectrum in p_T.

4.5 $\phi_B \to \phi_\mu$ Correlation Study

Especially important to any study of azimuthal particle distributions is modeling of the kinematic correlations between mother and daughter particles. A measurement of how the azimuthal angle relative to the reaction plane ϕ correlates before and after B meson decay would permit simulation of a flow signal parameterized by v_2^B, as is the goal in the next chapter. Since the MC Truth data created with Hydjet does not account for elliptic flow of heavy quarks, a straightforward measurement of v_2^B and v_2^μ for various values of v_2^B is not feasible. Instead, the measurement must be made on the kinematic level. In practice, this measurement was made by looping over known B/μ decay pairs in the MC Truth data and plotting histograms of ϕ_μ as a function of ϕ_B. Results for full-spectrum in p_T can be seen in Figure 4-6. Taking the difference $\phi_B - \phi_\mu$ gives a projection of the two-dimensional histogram along the $\phi_B = \phi_\mu$ line. The result in a Gaussian distribution, fit via a χ^2 method to determine RMS_ϕ, as shown in Figure 4-7 for full-spectrum in p_T.

39
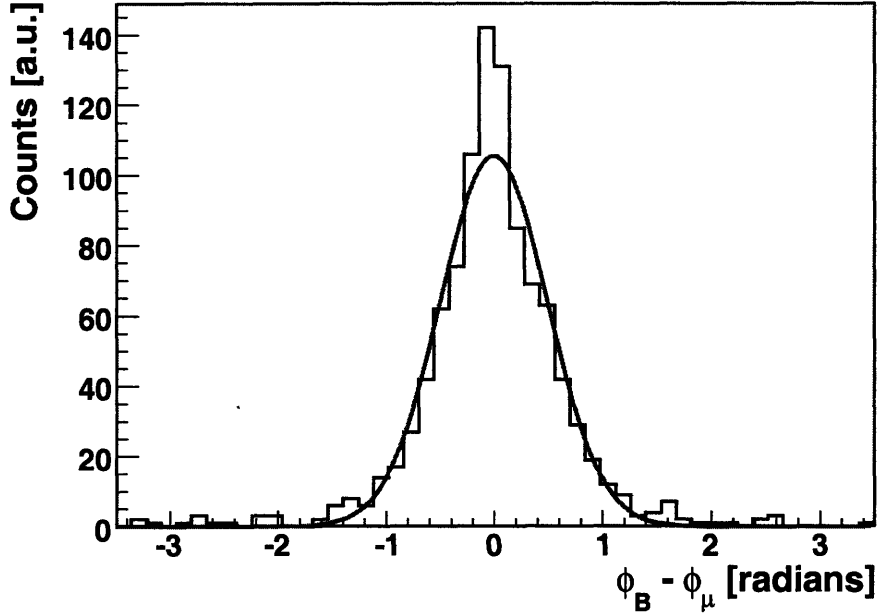
Figure 4-7: Histogram showing $\phi_B - \phi_\mu$ for all $B \rightarrow \mu^\pm$ mother-daughter pairs. This plot includes pairs from all values of p_T. Blue line is an example best-fit Gaussian.

Intuitively, any correlation between ϕ_B and ϕ_μ carries a p_T^B dependence: decays with greater boost in the transverse direction are more likely to produce a daughter close to the initial direction of travel (RMS$_\phi \rightarrow 0$). Conversely, B mesons at rest (i.e. $p_T = 0$) should emit daughter muons isotropically (RMS$_\phi \geq 2\pi$). To establish this relationship results similar to those described above were obtained for 1 GeV-wide bins in p_T^B up to 10 GeV, with a bin for p_T^B above 10 GeV ($\langle p_T^B \rangle = 12.68$ GeV). The results from each bin ranged between 30 and 180 decay products per bin, enough to be statistically significant. Gaussian fits were applied to each to obtain a value of RMS$_\phi$. Results can be seen in Figure 4-8. The data show the expected trend markedly well, allowing a fit such that RMS$_\phi(p_T)$ may be parameterized for later simulations. A weighted fit gives the functional form RMS$_\phi = 1.558(p_T^B)^{-.6415}$, where RMS$_\phi$ is in radians and p_T^B is in GeV.
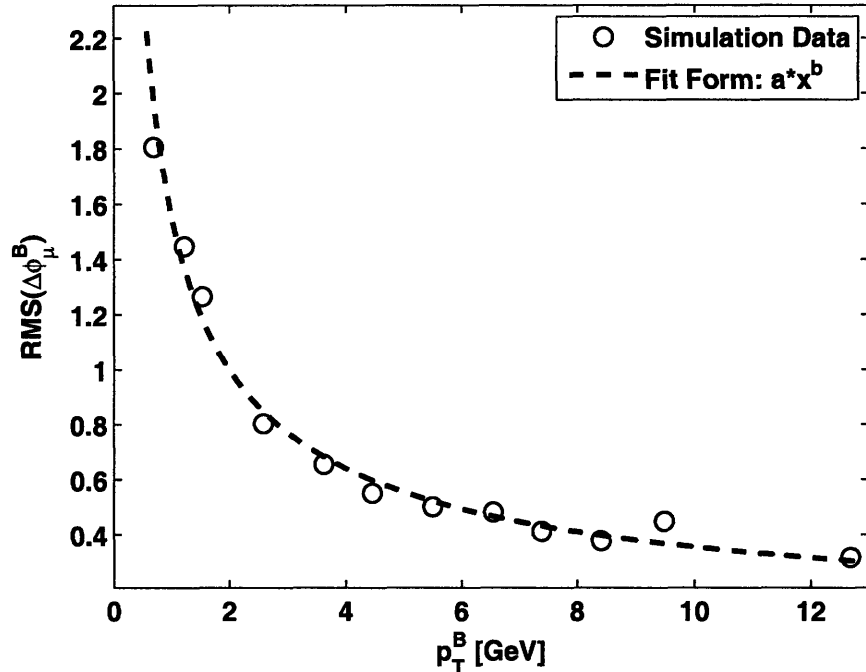
Figure 4-8: Plot of data correlating p_T^B to decay muon RMS$_\phi$, from MC Truth data. The dashed line is the best fit to the functional form $RMS = a * p_T^b$, with resulting parameters $a = 1.558$ and $b = -0.6415$. This functional form was used in the flow signal simulation study.

4.6 DCA Cutoff Study

Due to their finite, measurable decay length, it is possible to increase the signal to noise ratio of a study of heavy quark flavors by including only those particle candidates which originate from outside the central vertex. As mentioned in Section 3.3, the CMS silicon tracker will allow differentiation of particle vertices on distance scales fine enough to distinguish vertices most likely associated with charm decay from those most likely from beauty decay. This will further enable a study of open beauty flow alone, versus the combined heavy quark studies undertaken at RHIC. For the purposes of this analysis, an estimate of this cut would be useful to better establish an expected signal to noise ratio. This would also be useful later in actual CMS data analyses as a preliminary cut when analyzing initial B flow data.
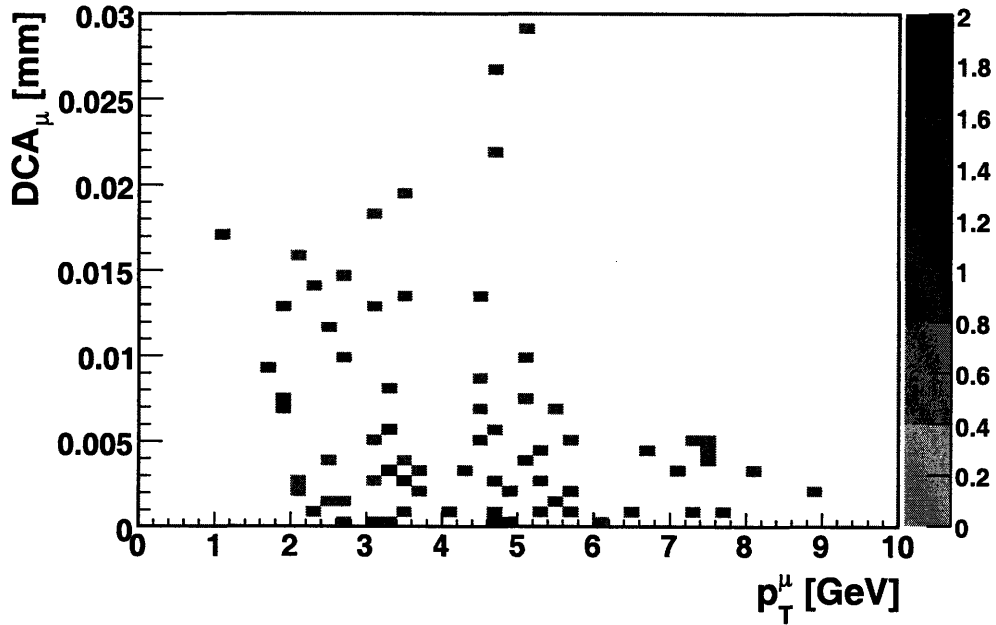
Figure 4-9: Two dimensional histogram of distance of closest approach values of B meson decay muons as related to p_T. Low statistics prevented this data from being used to recommend a DCA cutoff value for improving B decay measurements.

An attempt was made at establishing a best-fit vertex DCA cut using the Hydjet-generated MC Truth data along with RECO-processed data. First, full SIM and DIGI stages were applied to the MC Truth data, followed by running standard CMS Global Muon reconstruction. The software algorithm then looped over all reconstructed globalMuon candidates in an attempt to match the reconstructed muon track to an MC Truth muon candidate using kinematic parameters. Once the most likely match was found, the mother of the MC Truth particle was queried, and the muons were binned depending on whether they originated from a B meson or not. For both sets, the DCA and p_T of the muon were recorded and plotted. Results can be seen in Figures 4-9 and 4-10.

Unfortunately, the inavailability of CMSSW reconstruction algorithms compatible with heavy ion data hindered the success of this analysis. First and foremost was the inability of the muon reconstruction module to successfully process any data files for
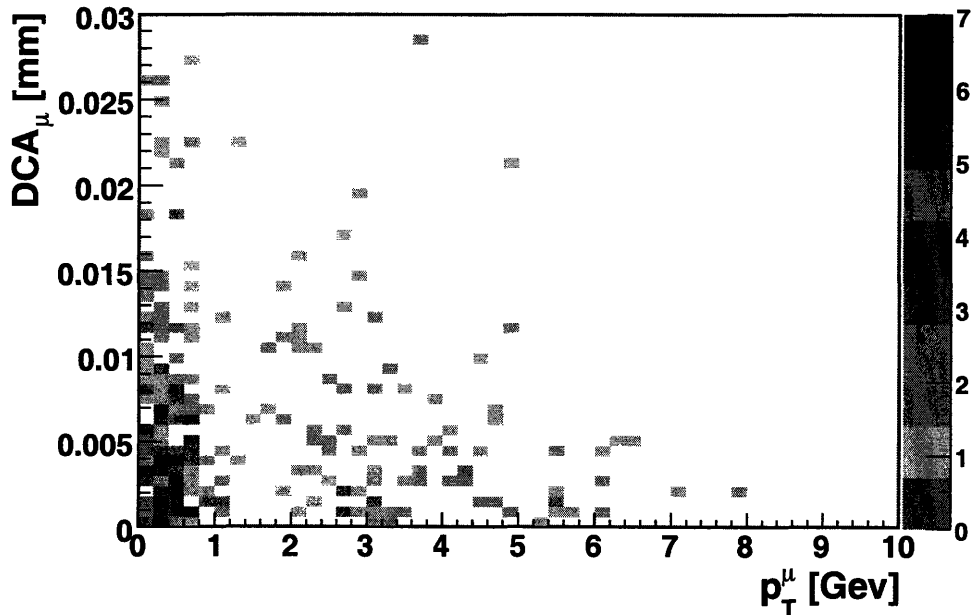
Figure 4-10: Two dimensional histogram of distance of closest approach values of background muons as related to p_T.

centralities other than $b = 12$. The root cause for this was likely in the sheer number of particles inherent to heavy ion collisions. The standard CMS muon reconstruction algorithm begins its analysis inside the tracker, where the high multiplicity of particles likely overloaded the algorithm [43]. Peripheral ion collisions were processable due to their many-times reduced multiplicity compared to central events. However, this inability to process three of the four data sets significantly reduced statistics to an unusable level. The data show no clear correlation between particle type and most likely impact parameter, preventing a best-fit for a DCA cutoff from being established. Due to this fact, any further analyses in this study will be parameterized according to an arbitrary DCA cutoff, with any conclusions made using simulated data from other experiments. Hopefully further studies will be possible once a muon reconstruction algorithm compatible with heavy ion data becomes available.

43

THIS PAGE INTENTIONALLY LEFT BLANK

Chapter 5

Flow Signal Simulation

Using the information learned from studying the MC Truth and RECO data, it is possible to construct a model flow signal to study how backgrounds affect statistical errors in the beauty flow measurement. The goal of this model is to produce hypothetical histograms of the Φ values of detected muons produced by open beauty in one month of heavy-ion data taking by the CMS detector. Estimates predict such a set of data to consist of approximately 10^7 min-bias events. This simulated data can then be fit to the functional form of an elliptic flow signal, making it possible to study how the properties of v_2 change as functions of the input parameters.

5.1   Method of Simulation

The signal histogram is created by employing a first-principles statistical method realized in a ROOT macro. The process loops over the requisite 10^7 events, performing the same set of randomized statistical processes on each.

First, an impact parameter for the event is pseudo-randomly selected according to the distribution given in Fig. 5-1, adapted from [44]. This distribution is an estimate of the cross section for each impact parameter in Pb + Pb collisions at LHC energies. This impact parameter is then used to determine the number of B mesons produced in the event N_B via the functional form shown in Figure 4-1. Usually this number is not an integer, in which case the macro produces enough B mesons to reach the

45

truncated integer value of N_B, then uses a less-than conditional comparison between the decimal portion of N_B and a flat random distribution to determine if an additional meson will be generated.
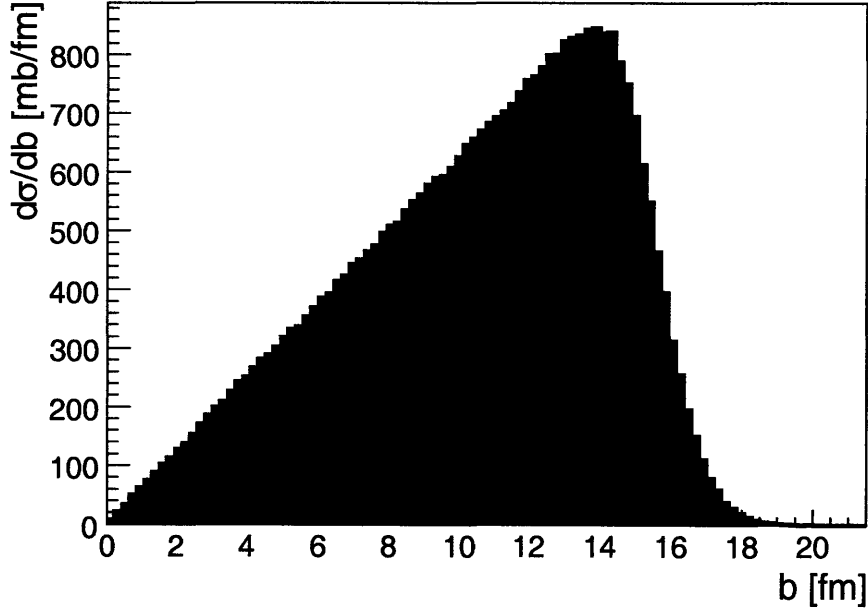
Figure 5-1: Distribution based on the multiple-scattering Glauber approximation of impact parameters for Pb + Pb collisions, normalized to total geometrical cross-section. Adapted from [44].

For each simulated B meson, relevant kinematic values were assigned. The macro pseudo-randomly assigns a transverse momentum value p_T^B using the distribution in Figure 4-2, and a azimuthal angle ϕ_B determined pseudo-randomly by a functional representation of a flow signal parameterized with a user-input value v_2^{IN}. For this study, values of $v_2^{IN} = \{.03, .05, .07\}$ were used due to their similarity to measured v_2 values for heavy quark flow [18]. Using the function determined by kinematic studies of MC Truth decay pairs, an RMS_ϕ is also assigned to each B meson based on the particle's given p_T^B (see Figure 4-8 for function and data). A less-than conditional comparison between the previously-measured muon production rate and a random number generator is then used to determine if each simulated B decays into a signal

muon. If it is the case that a muon is produced, the muon is assigned an azimuthal angle $\phi_\mu = \phi_B + G_B$, where G_B is a random number generated according to a Gaussian distribution with variance $\sigma^2_{gauss} = (RMS_\phi)^2$.
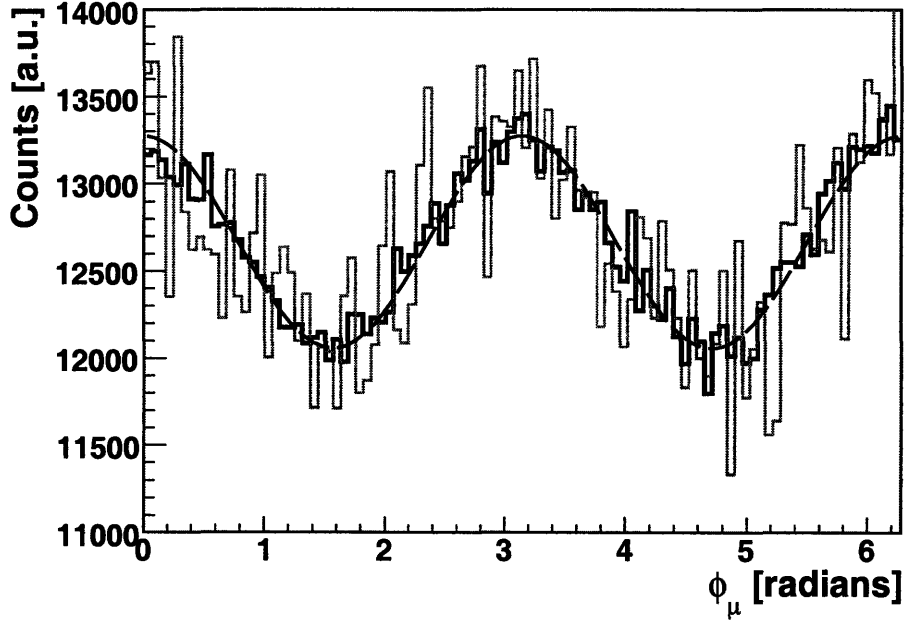
Figure 5-2: Plot showing example results from a single trial of the elliptic flow signal simulator. Blue histogram is the generated raw flow signal, with no background. Red histogram is the resulting flow signal after the addition of background, and subsequent subtraction of the constant average background rate. Black dashed line is the best-fit to the background-subtracted data. For this example, $N_{events} = 10^7$, $v_2^{IN} = .05$, $N_\mu^{back}/N_\mu^{sig} = 2.5$.

The simulated flow signal is generated when all values of ϕ_μ are histogrammed, as is shown in Figure 5-2. However, this would not be the signal observed in actual experiment: it is a pure signal, lacking any effects of background. To continue the study, a flat random background distribution is added to the histogram of ϕ_μ values. The ratio of background muons to signal muons $\frac{N_\mu^{back}}{N_\mu^{sig}}$ is specified as a parameter in the simulation. Studies of the MC Truth data determined this rate to be 1.875, however this study will explore values between zero and ten. Similar to experimental procedures, a constant distribution corresponding to the mean background level is then

subtracted from the combined signal and background data to produce a simulated data distribution. However, in practice the background would not likely be flat, but a simulated muon spectrum which includes other anisotropy and flow effects. Past experimental results of studies involving charm decaying to electrons have used such a Monte Carlo "cocktail" background simulation [9], with indications that using such a background would contribute a systematic error to measured v_2 results of slightly over 13%.

The resulting background-subtracted distribution in ϕ is then fit to the elliptic flow form to measure v_2^{fit}. An example simulated data distribution and fit are also shown in Figure 5-2. Varying the parameters of the study will then allow observations to be made regarding how the properties of B meson elliptic flow would impact the observed muon distribution in ϕ_μ.

For the following results, data points at specific values of v_2^{IN} and background level were established by iterating the macro 150 times for sets of 10^7 events each (except in cases where the number of events was purposely reduced). This was done to eliminate or characterize any sources of statistical error in the fitting and measurement process.

5.2   Simulation Results

The first results obtained using the flow signal simulation examined the relationship between $\left\langle v_2^{fit} \right\rangle$ and v_2^{IN} at different levels of background. When normalized for v_2^{IN}, the data were found to lie along a horizontal line for all explored values of v_2^{IN} and $\frac{N_\mu^{back}}{N_\mu^{sig}}$. These results can be seen in Figure 5-3. The mechanism behind this effect is the causal relationship between RMS_ϕ and how the flow signal is smeared by the B decay process. This measurement could change if a high minimum cut were placed on p_T^μ, implicitly choosing muons only from decays of B mesons with high p_T^B. The smaller RMS_ϕ of high-momentum decays would smear the flow signal less, resulting in a higher measurement. However, the higher cut would reduce the observed statistics of a real measurement.
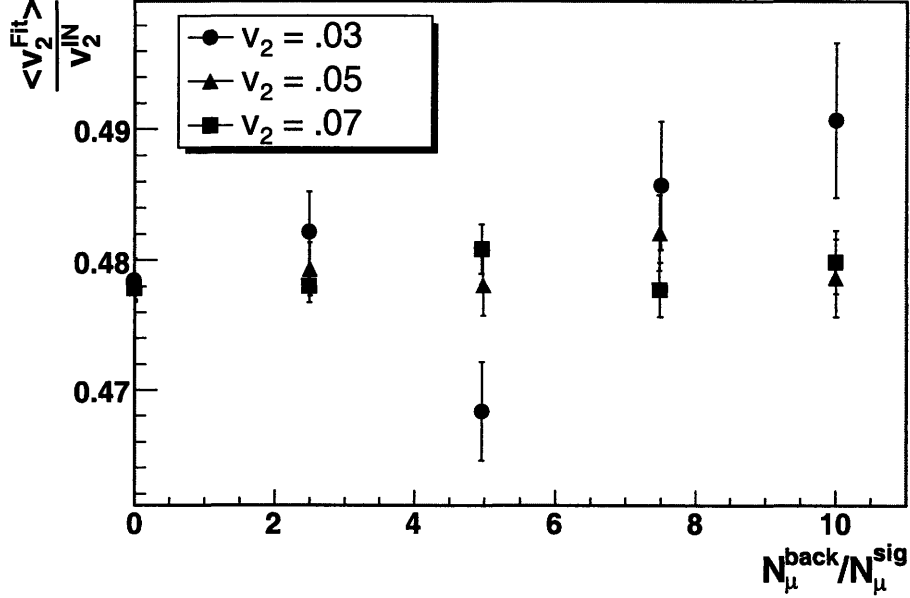
Figure 5-3: Data from simulated flow signal studies plotting $\left\langle v_2^{fit} \right\rangle$ for varying background levels, for three values of v_2^{IN}. Each data point represents 150 trials at the specified v_2^{IN} and background level. Error bars represent RMS_{v2} as measured by the ROOT Gaussian fitting algorithm.

The next set of results investigated how background levels might influence statistical variation in measurements of v_2^{fit}. For each of the 150 trials at a specific data point, v_2^{fit} was binned into a histogram. This histogram was then fit to a Gaussian form to determine the amount of statistical variations RMS_{v2}. The resulting data indicates a linear relationship between background level and RMS_{v2}, as shown in Figure 5-4. Data resulting from trials with all values of v_2^{IN} appear to fall along the same line. These results indicate that the precision of a measurement of v_2^B will not be dependent upon the real value of the B elliptic flow parameter, but rather more dependent upon the elimination or understanding of the contributions of background channels to the observed muon ϕ_μ distribution.

The final set of observations made using the flow signal simulator attempted to parameterize the response of RMS_{v2} as a function of the number of B decays observed. In a real experimental situation, this effect could arise from a number of sources; a
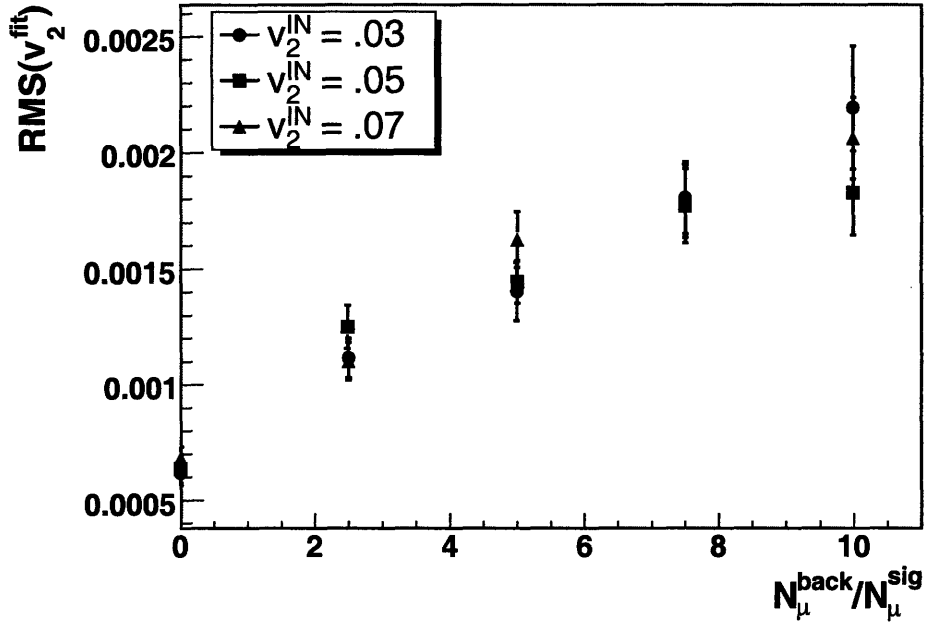
49

Figure 5-4: Data from simulated flow signal studies showing how RMS_{v2} changes for varying background levels, for three values of v_2^{IN}. Each data point represents 150 trials at the specified v_2^{IN} and background level. Error bars represent the confidence interval established by the ROOT Gaussian fitting algorithm.

lower luminosity in initial runs than expected, a suppression of b quark formation at high p_T, or a reduced set of desirable B decays following the application of DCA or kinematic cuts. Based on counting statistics, RMS_{v2} is expected to vary like $1/\sqrt{N_{event}}$. To mimic a reduced data set, the simulation macro was run with a reduction in the specified events N_{event}, down from the value of 10^7 used in previous studies. This is only one method by which this mechanism could be studied: variations could have been made to the function determining B meson production rates, allowing the effects of any uncertainty in measured cross sections to be investigated. Results from these trials are shown in Figures 5-5, 5-6, and 5-7. The data continue to exhibit the linear trend seen above for specific values of N_{event}. As N_{event} varies, the data show the expected trend, with RMS_{v2} increasing in a nonlinear fashion as N_{event} decreases towards zero. This effect will certainly have an effect on the precision of v_2^B if efforts to reduce background greatly diminish the size of the data set.

Figure 5-5: Plot showing the two-dimensional dependence of RMS_{v2} (z-axis) due to changes in N_{event} and background level, for $v_2^{IN} = .03$. Behavior along constant N_{event} is linear, while $\mathrm{RMS}_{v2} \propto 1/\sqrt{N_{event}}$. Data points interpolated with triangle mesh.
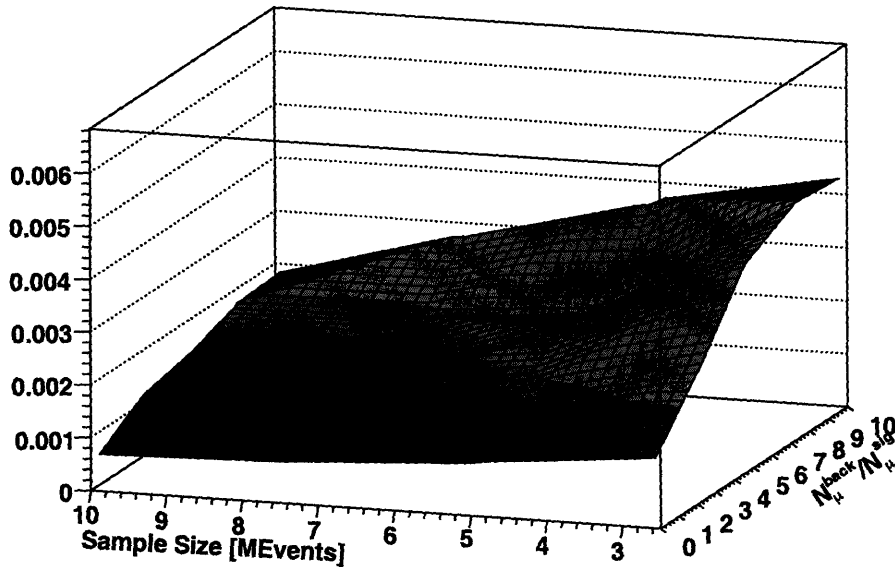
Figure 5-6: Plot showing the two-dimensional dependence of RMS_{v2} (z-axis) due to changes in N_{event} and background level, for $v_2^{IN} = .05$. Behavior along constant N_{event} is linear, while $\mathrm{RMS}_{v2} \propto 1/\sqrt{N_{event}}$. Data points interpolated with triangle mesh.
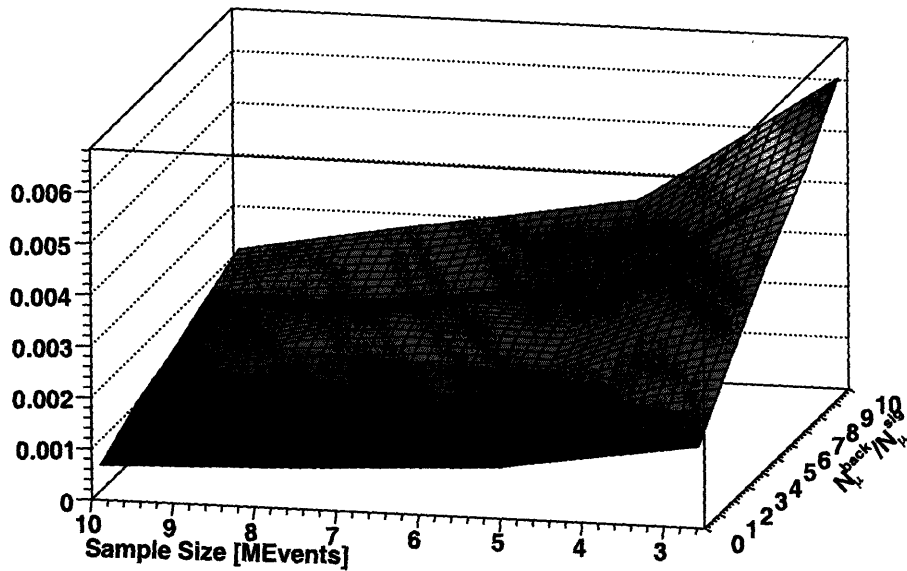
Figure 5-7: Plot showing the two-dimensional dependence of RMS_{v2} (z-axis) due to changes in N_{event} and background level, for $v_2^{IN} = .07$. Behavior along constant N_{event} is linear, while $\mathrm{RMS}_{v2} \propto 1/\sqrt{N_{event}}$. Data points interpolated with triangle mesh.
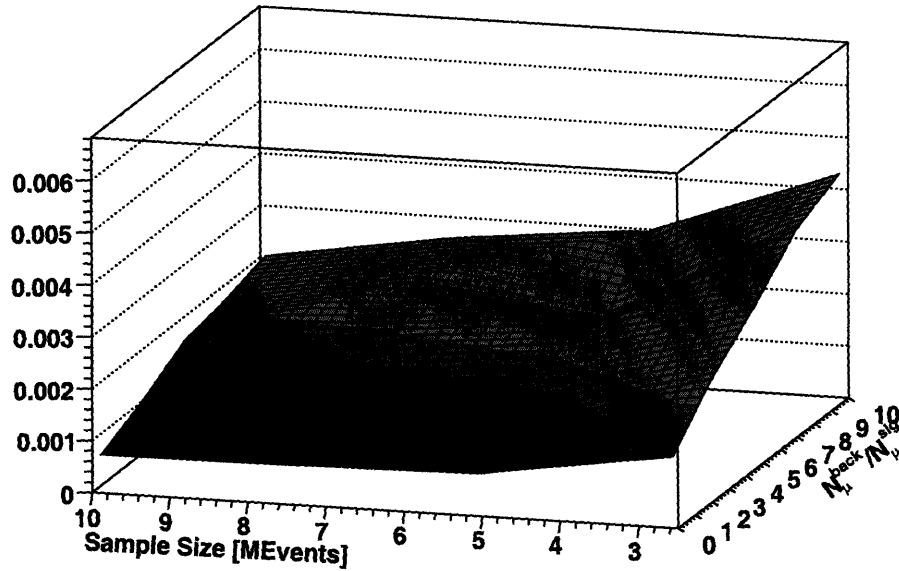
Chapter 6

Conclusions

When the LHC and CMS come online in the near future, physicists will have at their disposal the tools necessary to probe an energy regime never before explored. The field of heavy ion physics will be able to investigate new characteristics of the partonic QGP recently discovered at RHIC, including how b quarks form open mesons and flow within the elliptically-expanding QGP fireball. Since the B decay signal has never been seen independent of the effects of other quarks, and will play an important role in many related measurements, it is important that physicists take measures before first light of the experiment to understand how physical mechanisms will impact their expectations for results.

In this research, we attempt to understand and characterize the expected single-muon decay signal from elliptic flow of open beauty. Simulated Monte Carlo data was utilized to build the body of information necessary to produce a signal simulator. While attempts were made to characterize the DCA distributions and p_T^μ spectra of the signal muons, limited statistics proved to be insurmountable. However, the methods developed should be applicable and useful once a larger body of simulated data is available, or muon reconstruction within the CMSSW framework becomes potent with regards to central heavy ion data. Furthermore, since they were constructed within the CMSSW framework, all of the analysis tools used for these studies should be applicable to real experimental data when it becomes available, providing that some maintenance keeps the syntax of the code current.

The developed signal simulation tool was successful at producing data which will be relevant to future experimental studies. For simulated examples of elliptic flow within the realms of measured and predicted signal parameters, a number of measurement behaviors were characterized. It was found that v_2^μ is correlated to v_2^B by a constant linear relationship, with the correlation factor a constant for all potential values of v_2^B. In characterizing the statistical variation inherent to v_2^μ measurements of signal with background-subtraction effects taken into account, it was found that RMS_{v2} increases linearly with the ratio of background muons to signal muons. Choosing the background ratio $\frac{N_\mu^{back}}{N_\mu^{sig}} = 1.875$, as was determined from MC Truth data, the study yields a contribution to the statistical error in the measurement of v_2^B of $\mathrm{RMS}_v 2$ = 1.5% to 3% for v_2^B = .03 to .05. This can be compared to systematic contributions determined in [9] for charm studies of 3% (reconstruction efficiency) to greater than 13% (background subtraction assumptions), allowing the conclusion that studies of B flow using the CMS detector will not be hindered by statistical errors. Finally, it was shown that the size of the signal data set affects random statistical fluctuations of RMS_{v2} in a manner close to what is predicted by counting statistics. Due to the parametric nature of the simulation tool, it is foreseeable that future studies may make use of it to investigate the effects of nearly any change in the fundamental parameters of the flow signal.

Bibliography

[1] S.W. Herb et. al. Observation of a dimuon resonance at 9.5 gev in 400-gev proton-nucleus collisions. *Physical Review Letters*, 39(5):252–255, August 1977.

[2] A. Diamant-Berger et. al. Search for possible signatures of bottom-meson production in p-fe interactions at 400 gev/c. *Physical Review Letters*, 44(8):507–510, February 1980.

[3] A. B. Balantekin et. al. for the Particle Data Group. *Review of Particle Physics*, volume 33 of *Journal of Physics G*. Institute of Physics Publishing, Philadelphia, PA, July 2006.

[4] E. Norrbin and T. Sjostrand. Production and hadronization of heavy quarks. *European Physics Journal C*, 17:137–161, August 2000.

[5] M.C. Abreu et. al. for the NA50 Collaboration. Evidence for deconfinement of quarks and gluons for the j/ψ suppression pattern measured in pb-pb collisions at the cern-sps. *Physics Letters B*, 477(1-3):28–36, March 2000.

[6] A. Adare et. al. for the PHENIX Collaboration. J/ψ production vs. centrality, transverse momentum, and rapidity in au+au collisions at $\sqrt{s_{NN}} = 200$ gev. arXiv:nucl-ex/0611020v1, November 2006.

[7] E. Shuryak and D. Teany. J/ψ suppression in heavy ion collisions and the qcd phase transition. *Physics Letters B*, 430(1):37–42, June 1998.

[8] B. Povh et. al. *Particles and Nuclei: An Introduction to the Physical Concepts.* Springer, New York, NY, fourth edition, 2004.

[9] A. Adare et. al. for the PHENIX Collaboration. Energy loss and flow of heavy quarks in au + au collisions at $\sqrt{s_{NN}}$ = 200gev. *Physical Review Letters*, 98:172301, April 2007.

[10] A. Adare et. al. for the PHENIX Collaboration. Nuclear modification of single electron spectra and implications for heavy quark energy loss in au + au collisions at $\sqrt{s_{NN}}$ = 200 gev. *Physical Review Letters*, 96:032301, January 2007.

[11] B.I. Abelev et. al. for the STAR Collaboration. Transverse momentum and centrality dependence of high-pt non-photonic electron suppression in au+au collisions at $\sqrt{s_{NN}}$ = 200 gev. *Physical Review Letters*, 98:192301, May 2007.

[12] J. Richman and P. Burchat. Leptonic and semileptonic decays of charm and bottom hadrons. *Reviews of Modern Physics*, 67(4):893–976, October 1995.

[13] M. Djordjevic et. al. Open charm and beauty at ultrarelativistic heavy ion colliders. *Physical Review Letters*, 94:112301, March 2005.

[14] M. Hofmann et. al. *Nuclear Physics A*, 566(15c), 1994.

[15] J. Barrette et. al. for the E877 Collaboration. Observation of anisotropic event shapes and transverse flow in ultrarelativistic au+au collisions. *Physical Review Letters*, 73(19):2532, November 1994.

[16] H. Sorge. Elliptical flow: A signature for early pressure in ultrarelativistic nucleus-nucleus collisions. *Physical Review Letters*, 78(12):2309, March 1997.

[17] D. Teany et. al. Flow at the sps and rhic as a quark-gluon plasma signature. *Physical Review Letters*, 86(21):4783–4786, May 2001.

[18] S. Butsyk for the PHENIX Collaboration. Phenix results on open heavy flavor production and flow in au + au collisions at $\sqrt{s_{NN}}$ = 200 gev. *Nuclear Physics A*, 774:669–672, 2006.

[19] B. B. Back et. al for the PHOBOS Collaboration. Centrality and pseudorapidity dependence of elliptic flow for charged hadrons in au+au collisions at $\sqrt{s_{NN}} =$ 200 gev. *Physical Review C*, 72:051901, 2005.

[20] B. Alver et. al. for the PHOBOS Collaboration. Elliptic flow fluctuations in au + au collisions at $\sqrt{s_{NN}} =$ 200gev. arXiv:nucl-ex/0702036v1, February 2007.

[21] P. F. Kolb et. al. *Physical Review Letters C*, 500:232, 2001.

[22] J.F. Gunion and R. Vogt. Determining the existence and nature of the quark-gluon plasma by upsilon suppression at the lhc. arXiv:hep-ph/9610420v1, October 1996.

[23] Andrew M. Glenn. *Single Muon Production and Implications for Charm in sqrts$_{NN}$ = 200 Gev Au + Au Collisions*. PhD dissertation, The University of Tennessee, Knoxville, Department of Physics, December 2004.

[24] M. Lamont for the LHC Commissioning Working Group. Lhc - initial commissioning. http://lhc-commissioning.web.cern.ch/lhc-commissioning/presentations/co%mmissioning-stage-1.pdf, 2006.

[25] http://atlasexperiment.org/.

[26] http://aliceinfo.cern.ch/.

[27] http://lhcb.web.cern.ch/lhcb/.

[28] The CMS Collaboration. Csim drawing of the complete cms detector. Available: http://cmsinfo.cern.ch/outreach/CMSdocuments/DetectorDrawings/fromGEANT%/cms_complete_labelled.pdf.

[29] D. Acosta et. al. for the CMS Collaboration. *CMS Physics Technical Design Report, Volume I: Detector Performance and Software*, volume 8.1. CERN/LHCC, Geneva, Switzerland, 2 February 2006.

[30] M. Ballintijn et. al. Heavy ion physics at the lhc with the compact muon solenoid detector. http://yepes.rice.edu/cms/updateMay2003/CmsHiUpdate.pdf, May 2003.

[31] The CMS Collaboration. Cms muon technical design report. CERN/LHCC 97-32, http://cms.cern.ch/iCMS/jsp/page.jsp?mode=cms&action=url&urlkey=CMS_TDR%S, December 1997.

[32] R. Breedon et. al. Muon system performance studies for the cms technical proposal. CMS Technical Note 94-316, April 1995.

[33] M. Botenackels on Behalf of the CMS Collaboration. The cms muon spectrometer. From Beauty 2005 Proceedings, 2005.

[34] The CMS Collaboration. Addendum to the cms tracker tdr. *CMS TDR 5 Addendum 1*, February 2000. CERN/LHCC 2000-016.

[35] F. Hartmann on behalf of the CMS Silicon Tracker Collaboration. The cms all-silicon tracker – strategies to ensure a high quality and radiation hard silicon detector. *Nuclear Methods and Instruments in Physics Research A*, 478:285–287, 2002.

[36] M. Lenzi on behalf of the CMS Silicon Tracker Collaboration. Performance of the all-silicon cms tracker. *Nuclear Methods and Instruments in Physics Research A*, 473:31–38, 2001.

[37] Igor Lokhtin. Hydjet fast event generator. Available: http://lokhtin.home.cern.ch/lokhtin/hydro/hydjet.html, April 2007.

[38] Events generated by Yi Chen at MIT, Jan. - May 2007.

[39] http://cmsdoc.cern.ch/cms/sw/slc3_ia32_gcc323/cms/cmssw/CMSSW_1_3_2/doc/h%tml/.

[40] http://root.cern.ch/.

[41] N. Carrer and A. Dainese. Charm and beauty production at lhc. arXiv:hep-ph/0311225v1, November 2003.

[42] C. Blume and E. Vercellin for the ALICE Collaboration. Alice ppr volume ii, chapter 6.6: Quarkonia production. http://alice.web.cern.ch/Alice/ppr/web/PPRVIICurrentVersion.html, July 2006.

[43] K. Pernini et. al. Cmssw offline workbook: Global muon reconstruction. https://twiki.cern.ch/twiki/bin/view/CMS/WorkBookMuonGlobalReco, May 2007.

[44] Constantin Loizides. Heavy ion hlt timing studies. Available: http://www.cmsaf.mit.edu/twiki/bin/view/CmsHi/WebHome, April 2006.